A CMIP6 multi-model-based analysis of potential climate change effects on Kunhar River Basin, Pakistan

Engr. Abdul Waheed*[1], Dr. Muhammad Hidayat Jamal[2], Fawad Ullah[3], Muhammad Ameer Hamza[4], Dr. Khairul Idlan Muhammad[5] Muhammad Hammad[6], Dr. Muhammad Faisal Javed[7,10], Aitezaz Hassan Safi [8], and Ahmed Hussain[9]

[1]Sr.Engr.[7]Assist. Prof. Dept. of Civil Engineering, GIKi, Pakistan;
[10]Western Caspian University, Baku, Azerbaijan
[3,4,6,8,9] COMSATS University Abbottabad, Dept. of Civil Engineering 22060, Pakistan,
[2,5]Prof. Dept. of Civil Engineering, UTM, Malaysia,

awaheed@cuiatd.edu.pk, arbabfaisal@cuiatd.edu.pk, fawadktk778@gmail.com, hamza.zeb940@gmail.com, mh7097244@gmail.com, ahmadjadoon43@gmail.com, aitezazhassan0311@gmail.com , mhidayat@utm.my, mohdkhairulidlan@utm.my,

Abstract. Many of Pakistan's watersheds are facing challenges related to both water quality and availability, primarily due to changes in precipitation and temperature. This has prompted the need for revisions in management strategies. This research seeks to assess water security in northern Pakistan within the framework of anthropogenic climate change. The Kunhar River Basin (KRB), one of the biggest rivers in the region, was the subject of an analysis of the effects of Using Study how runoff is affected by climate change with the Soils and Waters Assessment Tool (SWAT).. Six general circulation models (GCMs), after bias correction, were used under two distinct emission possibilities for pathologies socioeconomically shared (SSPs). Nash-Sutcliffe effectiveness (NSE), percentage bias (PBIAS), and correlation coefficients (R2) were used to assess the model's performance, and the results showed that it performed better than 0.75. The results show that runoff in the KRB is well represented by the SWAT model at both the monthly and daily periods. The SSP2-4.5 and SSP5-8.5 scenarios predict an average annual increase in precipitation of 3.08% and 5.86%, respectively, over the 1980–2015 baseline.. It is also anticipated that daily high temperatures would increase by 2.08°C to 3.07°C, while average daily low temperatures are projected to increase by 2.09°C to 3.39°C from 2020 to 2099. As a result, annual runoff is projected to grow by 5.47% and 7.60% under the two

M. A. Tanoli et al. (eds.), *Proceedings of the 1st International Conference on Climate Change and Emerging Trends in Civil Engineering (CCETC 2024)*, Advances in Engineering Research 248,
https://doi.org/10.2991/978-94-6463-591-1_5

SSP scenarios, ensuring adequate water availability for future socioeconomic development.

Keywords: Climate change; Climate projections; Hydropower development; Kunhar River Basin; SWAT model; Trendanalysis.

1 Introduction

Floods are occurring more frequently in the lower Indus basin because river flows there correspond with the summer and rainy seasons, especially in Pakistan's Sindh region [1]. The impact of global warming on water availability must be continuously monitored and overseen in order to implement hydrological structures [2]. The predicted rise in global temperature may have an effect on hydrological cycles, which could cause disturbances to the current hydrological system [3]. The sixth assessment report from the IPCC presents a dire warning, stating that only considerable reductions in carbon emissions from this point forward can avert a worldwide environmental catastrophe should the world's temperature rise by 1.5 °C over the following two decades. 2020's Siberian heat wave and the Asian heat wave of 2016 might not have occurred if the world hadn't burnt through so much fossil fuel. [4]. The air can create roughly 4% more water for every degree Celsius of temperature rise, which can lead to heavy rains [5].

Pakistan was ranked as one of the top ten countries most susceptible to climate change by German Watch. (2019–20 Pakistan Economic Survey).The main cause of floods is heavy rainfall which increases the intensity of climate change. Pakistan's water resources managers and policymakers face a great deal of challenge as a result of the country's water problems [6]. In 1952, Pakistan's yearly water supply was 5,050 m3, but by 2006, it had dropped to 1,100 m3[7]. Because of the climate change, regional and temporal flow variability in the system is expected to vary, which will have a severe impact on the efficiency of these projects' costs [8].

The current study's focus, the River Kunhar, is a significant northern Pakistani catchment that supplies food to the country's agricultural and residential sectors. Babur et al. (2016) examined the KRB, tributary in Mangla River that provides water for five hydropower plants (HPPs) using a SWAT model.Among these, one is in the operational phase, while the remaining four are run-of-river HPPs in various stages of planning and construction [9]. Under both RCP 4.5 and RCP 8.5 scenarios, the mean annual flow exhibited an increase, with the winter and spring seeing the highest inflow and the summer and fall seeing the lowest.Three runoff river dams on the River Kunhar are in the planning stage, one is being built (883 MW Suki Kinari HPP), and the other is in operation (147 MW Patrind HPP). River Kunhar offers enormous possibilities for irrigation and power generation. Azim et al., 2016) [10] conducted a study on sediment movement in the Kunhar river basin, but few research have evaluated how climate change is affecting runoff. Shah and Ali, 2015 [11], Mahmood et al., 2016 [12]; Haseeb Akbar, 2020 [13]. Ali and Shah (2015) [11] used a snowmelt-runoff model to assess the basin

of the Kunhar River (KRB). They found that by the turn of the twenty-first century, there has been recorded increases in temperature of 2°C, rainfall of 20%, and discharge volume of 27%. The mean temperature series rises in the spring, falls in the warmer months of summer, and rises in the cooler months of fall and winter [9]. Hydrologic models, according to Weghost (1996) [14], Mukhopadyay (2015) [15], Lv, Z. et al. (2020) [16], Adnaan, M., et al. (2017) [17], and Musiee et al. (2020) [18], are essential for effective water resource management. (2017) Reggiani et al. [19] distinguished between hydrological models that are temperature- and energy-based, each of which needs a separate set of data to be used in simulationsRCP scenarios outperform SRES scenarios in terms of resolution and remove many of the latter's drawbacks.[20]. Given the current literature gap and the importance of this research in relation to various Sustainable Development Goals (SDGs), the objectives of this study is to investigate how the most recent CMIP6 scenarios would affect streamflow in KRB in northern Pakistan due to climate change. Potential repercussions of worldwide warming on water resources were evaluated utilizing the Water and Soil Evaluation Tool (SWAT), which included outputs from the CORDEX-South Asia climate model for both high-level (SSP5-8.5) and mid-range (SSP2-4.5) scenarios.

2 Data and Methodology: Study Area and Data:

Kunhar watershed is situated in northern Pakistan and covers an area of 2650 km^2 between 34.2° and 35.1° North and 73.3° and 74.1° East. Babosar Lake is the source of the River Kunhar, which flows to Mangla Reservoir before joining the Neelam River in Muzaffarabad (figure 1a). The largest tributary of the Kunhar River is 166 miles long, with its lowest point being 642 meters above sea level in the watershed, on the other hand 5106 meters its highest point is above sea level. elevation point. Originating from Lulusar Lake in the Kaghan Valley, the river traverses Bata Kondi, Jalkand, Kaghan, Naran, Balakot, Kawai, and Garhi Habibullah before ultimately meeting the Jhelum River near Rara. A prominent soil type known as leptosol medium (swat database code 3712) covers 75% of the basin, Combisole fine (swat code 3673) and Combisol medium (swat code 3672) make up 10% of the basin, and glaciers (swat code 6998) cover 5% of the basin. The soil types are shown in Figure 1(d). Just 3% of the basin's surface is covered by slopes ranging from 0 to 10%, whereas 42% is covered by slopes ranging from 30 to 60%. The Kunhar River's annual mean flow, as determined by the Ghari Habibullah stream gauge, was 102.6 m3/s. The climate data were collected from three meteorological stations: Narran, Balakot, and Muzaffarabad (table 1Until October 2020, the KBR's LULC is made up of a variety of ecosystems. To name a few, these are grazing, forested, snowy, and agricultural. (Figure 1c).

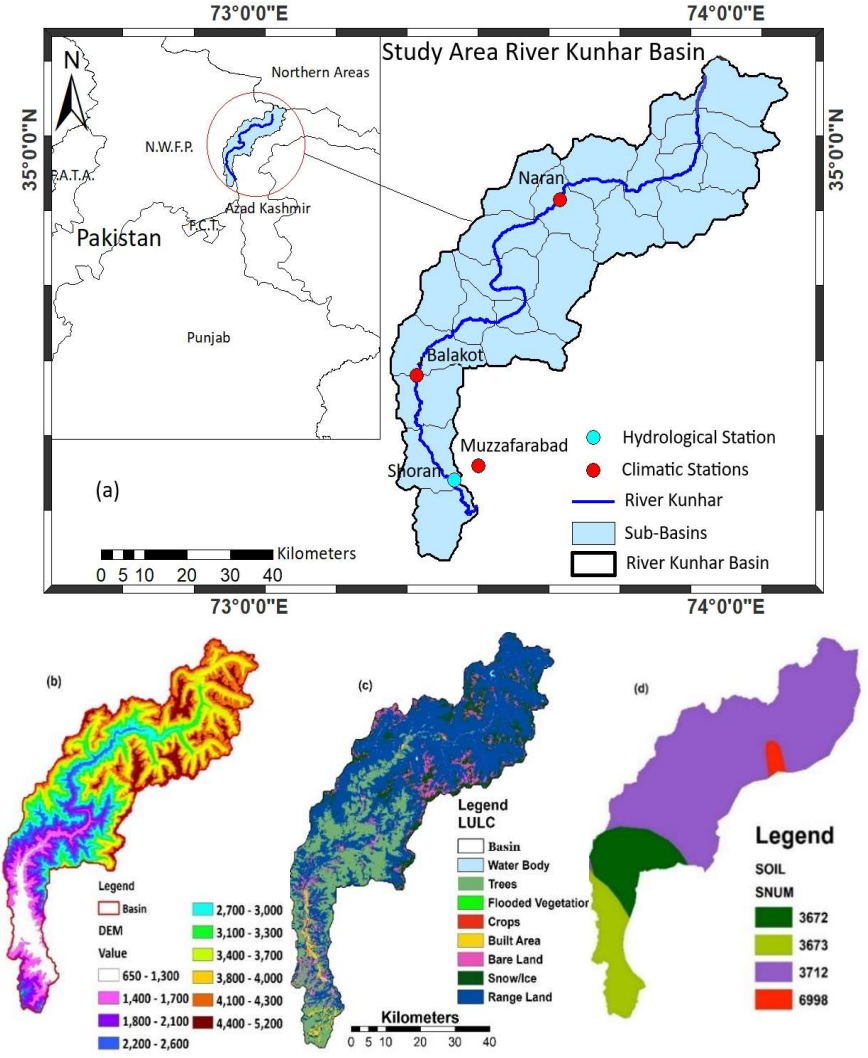

Fig. 1. Data inputs from SWAT. Area map (a), DEM (b), and LULC (c) (d) The KRB's soil classifications.

Table 1. KBR meteorological and hydrological data.

Station	Lat. (◦)	Long. (◦)	Altitude(m)	Record Duration	Data Source
Hydrological stations					
Shoran, Muzzaf-farabad	34.3	73.4	704	1971-2020	K-Water/ PMD
Meteorological stations					
Balakot	34.5	73.3	995	1971-2020	PMD
Muzzaffarabad	34.3	73.4	704	1971-2020	PMD
Naran	34.8	73.6	2422	1971-2020	PMD

2.1 Acquisition of Climate Data

To be employed, the SWAT model needs a DEM, a soil map, a land use/cover (LULC) map, and climatic data.ArcMAP10.3.1: The SRTM DEM (Shuttle Radar Topography Mission Digital Elevation Model) (figure 2b), which has spatial . The watershed of the KRB was delineated using a resolution of 30 x 30 m (Arc SWAT and its extensions are freely available from the website of the USDA-ARS). (https://swat.tamu.edu/software/arcswat/). Data about LULC was gathered from the ESRI. (Environmental Systems Research Institute) LULC database having spatial resolution of 10 x 10 m. The FAO World Data about soil was compiled using Soil Digital Map. Pakistan Meteorological Department (PMD) and Water and Power Development Authority (WAPDA) provided the daily climate statistics used to create the weather forecasts daily basis from 1961 to 2020 includes the highest (Tmax) and lowest temperatures (Tmin), precipitation observed at the Shoran station at two weather stations (Naran and Balakot), as well as flow discharge at Patrind Dam. Figure 2 shows the historical data from 1960 to 2020.

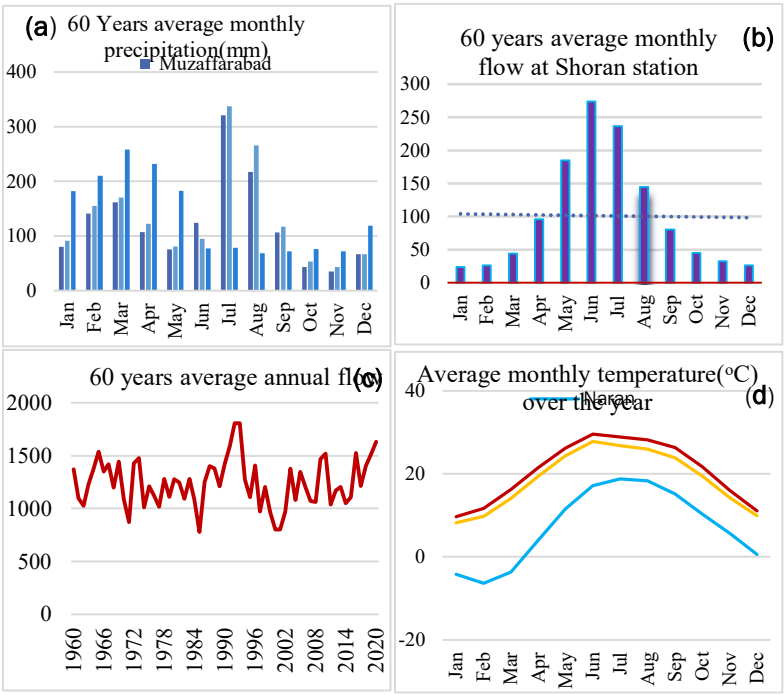

Fig. 2. Average year-over-year variations in KRB the Kunhar watershed's average monthly temperature over three meteorological stations, a) monthly PPT on average, b) monthly flow on average, c) the average annual flow changes over 60 years, and d) average monthly temperature.

2.2 Climate data collection

This study utilized the SWAT model and six downscaled, bias-corrected General Circulation Models (GCMs) to investigate how climate change affects the KRB's discharge. During the investigation, two Shared Socioeconomic Pathway (SSP) SSP2-4.5 and SSP5-8.5 situations were taken into account. Predicted climate data was obtained using nine general circulation models. Projections from the Earth System Grid Federation (ESGF) and the Climate Change Knowledge Portal (CCKP) were analyzed to determine how precipitation, maximum, and minimum temperatures will change over the next decades. Data extraction was followed by bias adjustment for the future. For bias correction, the CMhyd software used the linear scaling (L.S) approach. Equations 1 and 2 contain the equations for the ppt's bias correction. Equations 3 and 4 also serve as mathematical models for the correction of temperature bias. Several climate studies (Akbar and Ghewala 2020[21], Lafoon et al. 2013 [22]) have effectively employed this methodology.

Precipitation

P+h=Ph(d)am(P_ob (𝑑))/am(P_h (d)) (1)

P+f=Pf(d)am(P_ob (𝑑))/am(P_h (d)) (2)

Temperature

T+h = Th(d) + am (Tob(d)) – am (Th(d) (3)

T+f = Tf(d) + am (Tob(d)) – am (Th(d) (4)

Where P depicts precipitation, T symbolizes temp; h = historical; ob is used for observational The bias-corrected data is shown as run, f=future run, a = average, d = day, m = monthly,, +.

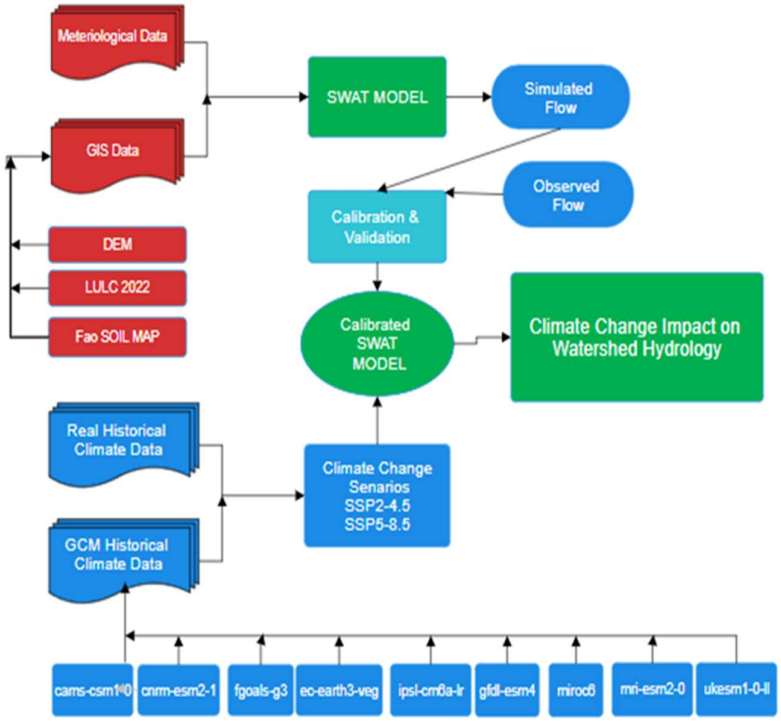

Fig. 3. An illustration of the methodology used in this study.

2.3 SWAT Model

The initial goal of SWAT, a physical-based continuous-time model based on river basin and semi-distributed processes, was to predict the long-term impacts of land-use management practices and climate change on water, agricultural chemical outputs, and sediments in composite river basins ranging in size from moderate to large ([23], [24]). Watersheds are divided by SWAT into smaller simulated regions known as hydrological response units (HRUs) according to

the types of soil, slope classes, and land uses. Through the solution of the water balance equation, which takes into account daily variables including percolation, precipitation, evapotranspiration, runoff, and return flow, the model forecasts hydrology for each Hydrological Response Unit (HRU). Two methods are used by the model to forecast surface runoff: The methods that are being discussed are (a) Green and Ampt and (b) Natural Resources Conservation Service Curve Number (CN) method. To predict the percolation over each soil layer, storage routing methods are used with a crack-flow model. To calculate the flow routing in river channels, the Muskingum method, also known as the adjustable storage coefficient methodology, is utilized ([23],[24]). The conceptual foundation for the model's application is the water balance equation [25].

$$SW_t = SW_0 + \sum_{i=1}^{i} \left(R_{day} - Q_{surf} - E_a - W_{seeP} - Q_{gw}\right)$$

In this scenario, Wseep denotes the depth of soil flow on day i, Qgw denotes the depth of groundwater runoff on day i, Rday denotes Day I precipitation, Day II surface runoff I is shown by Qsurf. Ea stands for evapotranspiration on day i, and t denotes time. Millimeters are used to measure water, whereas days are used to measure time…….

2.4 CONFIGURATION OF THE MODEL

The following procedures were engaged in creating the SWAT model: (i) Developing DEM, delineating watersheds and sub-watersheds; (ii) Analyzing Hydrological Response Units (HRUs) and elevation bands; (iii) creating a map of the soil; (iv) running the model and setting its parameters; and (v) Conducting calibration, validation, and uncertainty analysis. (Figure 4). The SWAT model at Shoran station was installed using the same methodology that proved successful In past studies (Ahmed et al. 2012 [26]; 2013 Reh¬man et al. [27]; 2014 Haguma et al. [28]; 2014 P.J.Y and R.A.Km [29]; 2019 Koycigiz and Buy¬okyildiz [30]; 2019 Shange et al. [31]; Haidar et al. 2020[32]; Musiee et al. 2020 [18]). The SWAT model simulates two key phases of the hydrological process: runoff generation and overland flow concentration. In this study, the Kunhar River Basin (KRB) was divided into 277 hydrological response units ((HRUs), as well as twenty-three sub-basins analysis.

2.5 General Circulation Models and Climate Change Scenarios

After comprehensive literature review and applicability of CMIP6 in Pakistan [33, 34], six CMIP6 global climate models were based on their spatial resolution, the following datasets were chosen for comparison in this study: : cams-csm1-0, cnrm-esm2-1, ec-earth3-veg, mri-esm2-0, fgoals-f3, ukesm1-0-ll; two SSP emission scenarios were used to model potential discharge in the future: SSP2-4.5 and SSP5-8.5. The model's name and key characteristics are listed in Table 2. The representative concentration pathways (RCPs) for CMIP5 are replaced by shared socioeconomic pathways (SSPs).

The primary difference between SSPs and RCPs is the combined trajectories for gaseous emissions, such as carbon dioxide.

Table 2. Details of the six GCMs used in CMIP6.

Sr. No	GCM	Country	Institution	Resolution
1	Cams-csm1-0.	China	Beijing's Chinese Academy of Atmospheric Studies	1.1° x 1.1°
2	cnrm-esm2-1	France	The Center for National Meteorological Research (CNRM)	0.5° x 0.5°
3	ec-earth3-veg	Sweden	EC-Earth consortium, Rossby Center, , Sweden	0.7° x 0.7°
4	fgoals-g3	China	Academy of Sciences in China, Beijing, China	1.3o x 1.0o
5	Mri-esm2-0.	Japan	Japan's Meteorology Research Center (MRI) is located in Tsukuba, Ibaraki	1.1° x 1.1°
6	Ukesm1-0-ll.	UK	Exeter, UK's Met. Office Hadley Center	1.9° x 1.3°

3 Results and Discussion

3.1 Sensitivity Analysis of Variable Parameters

Hydrological model applicability can be tested, and parameter sensitivities examined with the use of SWAT-CUP's SUFI-2 algorithm. Based on the literature [32], [35], [36] Thirteen of the most sensitive parameters were found using SWAT-CUP and are included in the Table 3. Model parameters were tuned by repeated simulations employing the SUFI-2 technique in order to attain optimal outcomes. For this, we employ the t- data and corresponding p-value indicating that SUFI-2 method generates. The parameters may be more sensitive if the t-Stat value is higher. The p-value indicates the significance of sensitivity. The significance of the sensitivity increases as the p-value approaches 0 (Table 3) [35, 37].

Table 3. Variety for delicate parameters in the discharge process for model calibration..

Num	Parameters	Description	t-Stat	p-Value	Value Adjusted	Max & MinValue
1	v_ESCO.hru	Factor for Soil Evaporation Compensation	-13.89	0.015	0.851	0.8 – 1
2	v_CH_N2.rte	For the channel of communication, the Manning n coefficient	-4.125	0.021	0.112	0 - 0.3
3	v_SLSUBBSN.hru	Median slope length	-4.052	0.055	49.51	10 - 150
4	v_GW_DELAY.gw	Groundwater delay	-1.632	0.070	115.85	0 - 500
5	v_ALPHA_BF.gw	Base flow's alpha factor	-1.562	0.073	0.44	0 – 1
6	v_SMFMX.bsn	Snowmelt factor	-1.585	0.078	4.21	0 – 20
7	v_CH_K2.rte	Hydrostatic conductance of the main conduit	-1.523	0.115	25.65	5 - 130
8	v_GWQMN.gw	The minimum depth of water required for the return flow in a shallow aquifer	-1.466	0.118	1800	0 - 5000
9	v_SMTMP.bsn	Warmth of the snow's base dissolving	-1.432	0.125	9.85	−20 - 20
10	r_SOL_K (1).sol	Hydraulic soil saturation	-1.365	0.146	0.65	-0.8 – 0.8
11	r_SOL_AWC (1).sol	The ability of the top layer of soil to retain water	-0.885	0.322	-0.11	-0.2 – 0.4

12	v_GW_REVAP.gw	Ground-water re evaporation coefficient	-0.756	9	0.53	0.098	0 - 0.2
13	r_CN2.mgt	Curve number	-0.652	1	0.60	-0.172	-0.2 – 0.2

3.2 SWAT Model Applicability Analysis.

The accuracy of the hydrological models was assessed using a R2 statistic, % distortion (PBIAS), or Nash-Sutcliffe productivity (NSE). The extent of the relationship between the model and observed data is shown by the R2, or degree of correlation. The level of conformity among the predicted and reality lines is displayed by the NSE. Less inaccuracy is shown by higher R2 and NSE numbers (which vary from 0 to 1). Both the usual slope of the simulated flows and the typical percentage variation between the simulated and actual flows are shown by the PBIAS. A positive number indicates an underestimation and a negative value indicates an overestimation; the permissible range for PBIAS values is -15% to 15%. (Gheewala and Akbar, 2020 [38]). NSE is used to assess how well a model replicates patterns in a significant output response over time that have been observed [39].

$$NSE = \left[1 - \frac{\sum_{i=0}^{n}(Q_{o.i} - Q_{s,i})^2}{\sum_{i=1}^{n}(Q_{o,i} - Q_{o,m})^2}\right]$$

$$Pbias = \left[\frac{\sum_{i=0}^{n}(Q_{o,i} - Q_{s,i})}{\sum_{i=0}^{n} Q_{o,i}}\right] * 100$$

$$R^2 = \left[\frac{\sum_{i=1}^{n}(Q_{o,i} - Q_{o,m})(Q_{s,i} - Q_{s,m})}{\sqrt{\sum_{i=1}^{n}(Q_{o,i} - Q_{o,m})^2}\sqrt{\sum_{i=1}^{n}(Q_{s,i} - Q_{s,m})^2}}\right]$$

The value "n" in equations 2, 3, and 4 refers to the total quantity of observed and simulated pairings. Specifically, Qo represents the observed flow, Qs the simulated flow, Qo,m the average observed flow, and Qs,m the simulated average flow. The observed and anticipated discharges during the calibration (1990-2010) and validation (2011-2020) phases show good correlation, as shown by the daily and monthly time series plots (Figures 4). Using flow duration curves—which can be generated from simulated or observed data using hydrologic models—high, medium, and low flow rates are comparable [40]. Figure 6 displays the daily and monthly discharge curves representing the flow time for the base period 1990 to 2020 respectively. There is a good match between the predicted and actual daily discharge, but there are instances where either too excessive or insufficient for peak discharges. The daily and monthly flow duration curve in Figure 6 (a,b) demonstrates that most of the high flows (>100 m3/s) were over-simulated. Most of the small flows are underestimated. Table 4 provides an overview of the important performance metrics derived from the daily and monthly discharge simulation results of the SWAT model. The equivalent R2 values for the daily discharge simulation are 0.88 and 0.90, and for both the calibration and validation periods, the NSE values are more than 0.75.. In comparison to the daily

discharge simulation, the NSE, R2, and KGE values of the SWAT model are much greater for the monthly discharge simulation.

Table 4. The calibration and validation performance indicators of the SWAT model

Temporal Scale	Period	NSE	R^2	PBIAS
Daily	Calibration	0.80	0.80	-6.53
	Validation	0.81	0.82	-6.33
Monthly	Calibration	0.82	0.81	-6.08
	Validation	0.83	0.83	-6.73

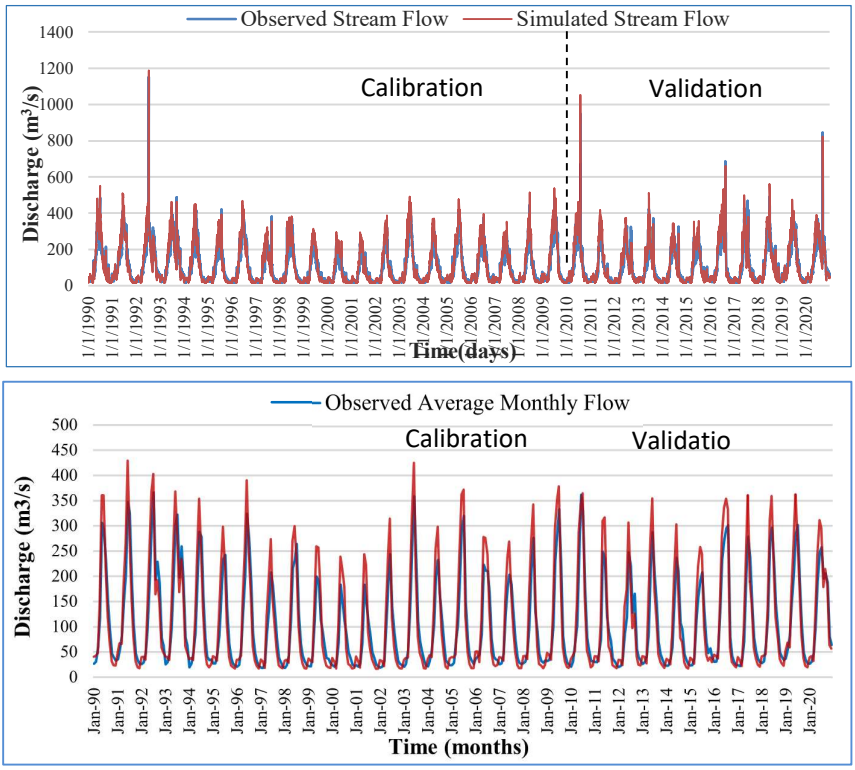

Fig. 4. Daily discharge during the calibration and validation periods compared to the simulated values.

3.3 Future Temperature and Rainfall Projections

Rainfall variability is a good indication of climate change because it has an immediate influence on the procedure of runoff and the hydrological cycle [41]. For the reference period, the average annual rainfall was 1597.20 mm. The results for SSP2-4.5 and SSP5-8.5 in relation to the baseline are displayed in Figure 7. More than half of the

GCMs indicate an increase in precipitation under the SSP2-4.5 emission situation, with projections that vary from a low of -9.23% to a high of 21.12% for the years 2021–2099. The range of predicted values for precipitation increases for the The lowest predicted number for the SSP5-8.5 emission scenario is -10.45%. The emission scenario is (-0.354%, 11.254%) and the largest rise being 24.63% across all GCMs. Although it does show an upward tendency, the average amount of precipitation each year in the KRB differs very little amongst SSP scenarios (Figure 9). Six GCMs were used to simulate monthly increases in precipitation for the two SSPs scenarios in order to assess near, mid, and long-term projections. The percentage changes in precipitation for the short, mid, and long term across all six General Circulation Models (GCMs) are shown in Figure 8. Under SSP 2-4.5 emission circumstances, there would be a 50% decrease in the early fall season and rises of up to 28% in the mid-future and 40% for the early monsoon season in the far-future, precipitation increases dramatically in warm weather and in the late autumn when utilizing CAMS-CSM1-0. Though the hot time is expected to reduce by 39% according to CAMS-CSM1-0 over the long future and a In the early forecast era, there was a 45% increase. The SSP5-8.5 emissions scenario, early monsoon precipitation is projected to increase by 45% in the near future. For the mid and distant future, climate models such as MRI-ESM2-0, MIROC6, and UKESML-0-LL predict a 35% increase in warm weather. These changes are within the SSP5-8.5 scenario framework. Watershed data suggests that we can expect an increased snowfall during the winter months and a rise in the quantity and severity of wet precipitation throughout the rainy season [42]. Annual maximum temperatures average 20.63 oC, while low temperatures average 12.19 oC for the baseline. The comparison examines the differences in the annual mean high and low air temperatures for the baseline period of 1990-2020 under the two SSPs emission scenarios (Figure 8). Future projections indicate that the KRB's mean temperature will rise noticeably. Over the coming decades, all six GCMs predict an increase in the lowest and most extreme air temperatures. (Figure 8). The maximum air temperature will rise by an 2.09°C on average, with a 1.39°C range to 2.83°C, under SSP2-4.5 emission scenario, whereas the maximum air temperature would rise by 3.07°C under the SSP5-8.5 emission scenario, ranging from 1.60°C to 4.15°C. Temperature and precipitation records indicate that the Kunhar River Basin (KRB) is expected to continue experiencing hot, humid hydrothermal conditions in the future.

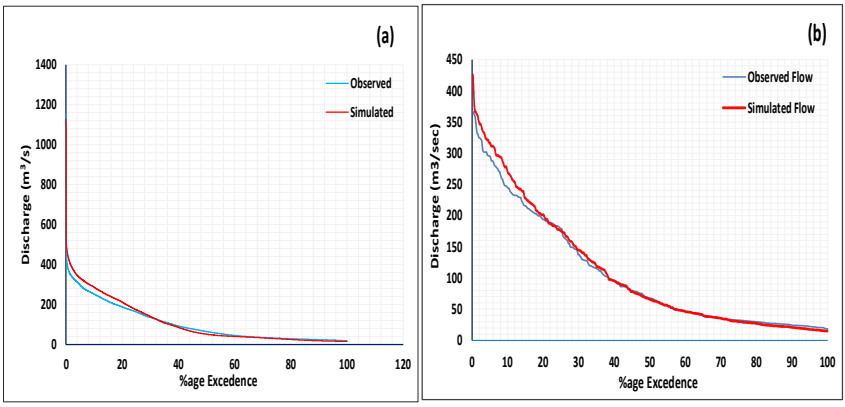

Fig. 5. Catchment flow duration curves on a) Daily basis. b) Monthly Basis.

3.4 The effects of climate change on runoff.

The Kunhar River Basin projected seasonal and annual streamflow was compared to the historical period. Forecasted annual flow percentage changes (Figure 11) by all six The discharge is expected to grow by an average of 5.42%, according to GCMs. and (Under the SSP2-4.5 emissions scenario, 25% to 75% of the values from all GCMs are projected to range between 1.90% and 9.04%, with an average value of 7.60%. Meanwhile, for the SSP5-8.5 scenario, 25% to 75% of values will fall between 1.51% and 13.08%. Figure 12 illustrates the average monthly and seasonal variability in runoff for the Kunhar River Basin (KRB) from 2021 to 2099. Under the SSP2-4.5 emission scenario, the peak monthly discharge values vary from 368.74 m3/s in 2099 to 271.22 m3/s in 2059, with 2099 having the largest runoff. With the SSP5-8.5 emission scenario, the average monthly maximum runoff increases to 387.54 m3/s in (2020–2039). Compared to baseline, it's more likely that the ec-earth3-veg model will anticipate higher winter and spring flows than a significant decrease in summer flows.

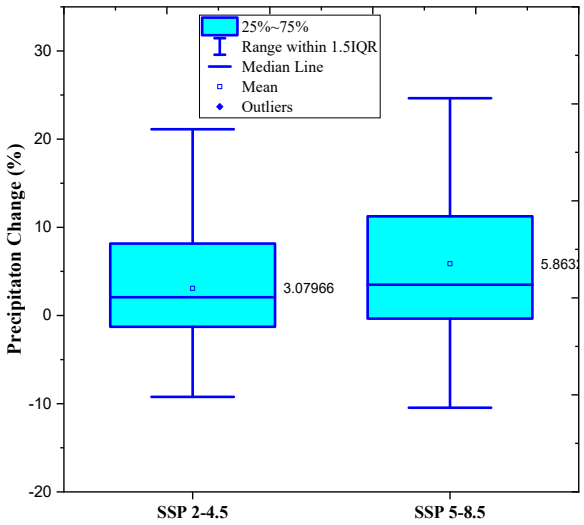

Fig. 6. The boxplot displays the percentage changes in SSP2-4.5 and SSP5-8.5 precipitation across six different GCMs in comparison to the baseline period.

Regarding the SSP2-4.5 emission case, CAMS-CSM1-0 projected future rises of up to 41.70%, and for the SSP5-8.5 scenario, up to 43.92%. The peak flow was found to be shifting to early summer in ec-earth3-veg, mri-esm2-0, and CAMS-CSM1-0, whereas it appeared to be shifting June through July and August in fgoals-g3. Ultimately, in all reliable approximations, the rates of increase in flows surpass the rates of reduction. Flood levels in the KRB may rise significantly in the future compared to previous times, figures 9 and 10. show the average annual streamflow fluctuations by climate change for the KRB. The yearly runoff is expected to increase by 10% Under the SSP2-4.5 conditions and by 19.50% in the SSP5-8.5 scenario. By the middle of the century, yearly runoff falls by 11% in the SSP2-4.5 scenarios and increases by 11.5% in the SSP5-8.5 scenarios. Discussion TIt is discovered that the flow forecasts for the climate conditions are sensitive to the parameters of the climate forecast and modeling, indicating the value of cross-referencing our findings with those of previous studies conducted in the same basin. Earlier research thus turned out to be the most beneficial for our investigation. With the use of distinct hydrological models and climatic data, each study produced wildly disparate future projections. Baber et al. (2016) [9] showed that river flows are highest in the spring and lowest in the winter. Mahmod et al. (2016) [43], however, found an opposite tendency while examining the yearly mean flow throughout various seasons. Ghulam Nabi et al. (2022) [44] forecast the average flow annually at Ghari Habibullah will increase between 2021 and 2040, decrease between 2041 and 2070, and then increase again between 2071 and 2099. Our findings more closely resemble those of Ghulam Nabi and colleagues (2022)[44] nevertheless, we utilized

CMIP6 models, which offer enhanced representation of physical, chemical, and biological processes and greater spatial resolution compared to the CMIP5 models (Stouffer et al. 2017; Zhu & Yang 2020) [45]. It is challenging to forecast future modifications in the flow regime because varying research has different baseline periods. While Mahmod et al. (2016) [43] revealed that the baseline flow (25 m3/s) would vary by 2%, 11%, and 2% in the near, medium, and far futures, respectively. Babar et al. (2016) [9] predicted that baseline flow (26 m3/s) would increase by 44.12%, 69.11%, and 110.9% in the futures—near, medium, and far for the RCP 8.5 scenario. The specifics of the climate data and calibration parameters used to create hydrological model projections are crucial. In the near, mid, and far future times, correspondingly, by mri-esm2-0, the highest percent change in winter flows was found to be 76.56, 77.24, 61.28, and 29.50 by our research under the SSP2-4.5 emission scenario. In contrast, the emission scenario for SSP5-8.5 reflects 10.22, 3.56, 24.67, and 51.44 percent modifications for corresponding future winter flows.

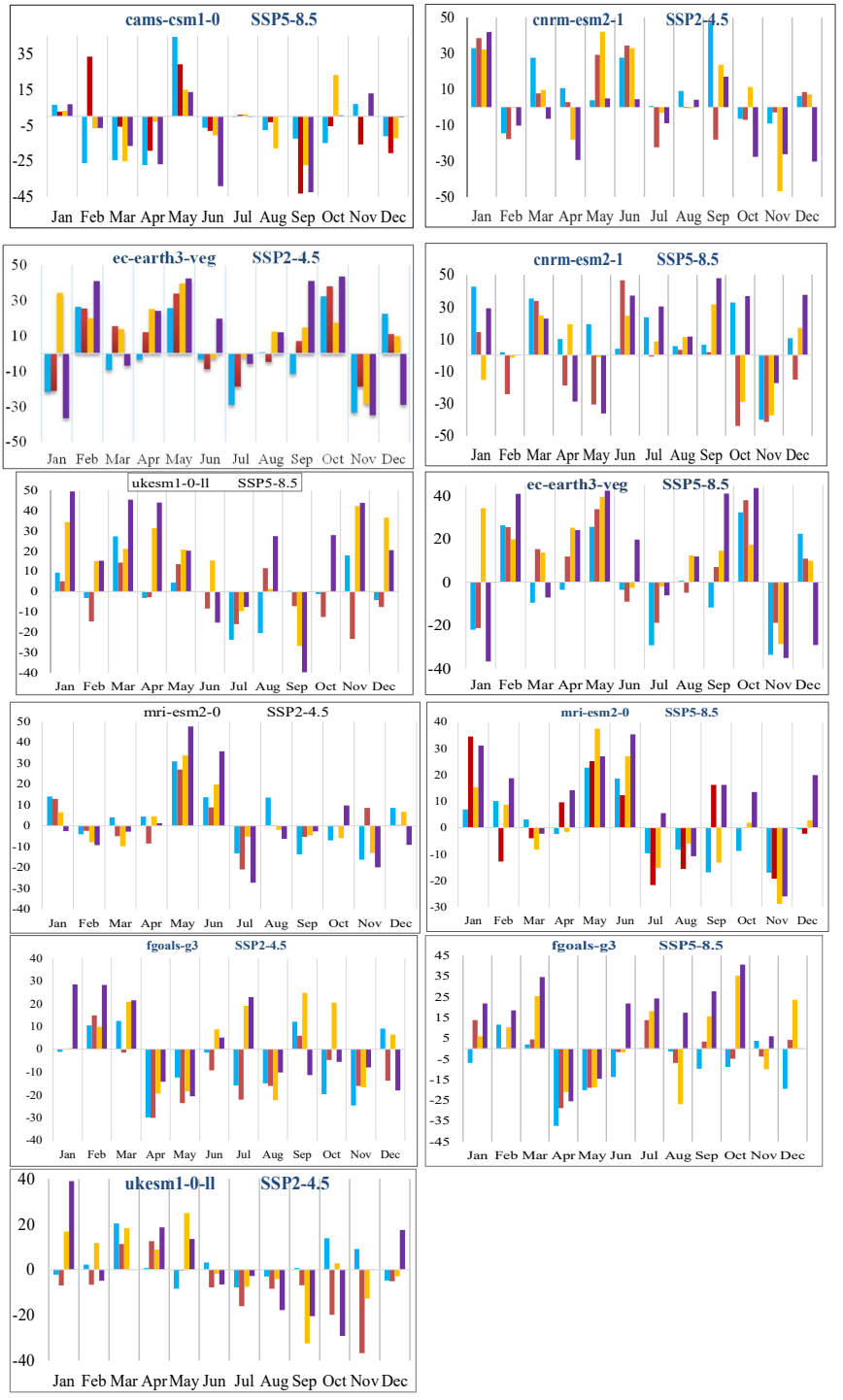

Fig. 7. The anticipated change (% change, y-axis) in yearly precipitation between 2021 and 2099.

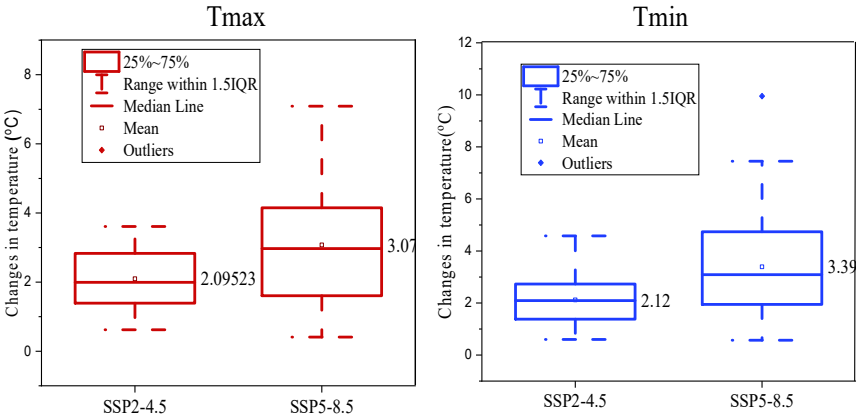

Fig. 8. The temperature variations of nine GCMs are displayed in the box plot under SSP2-4.5 and SSP5-8.5, respectively, for the maximum and lowest temperatures.

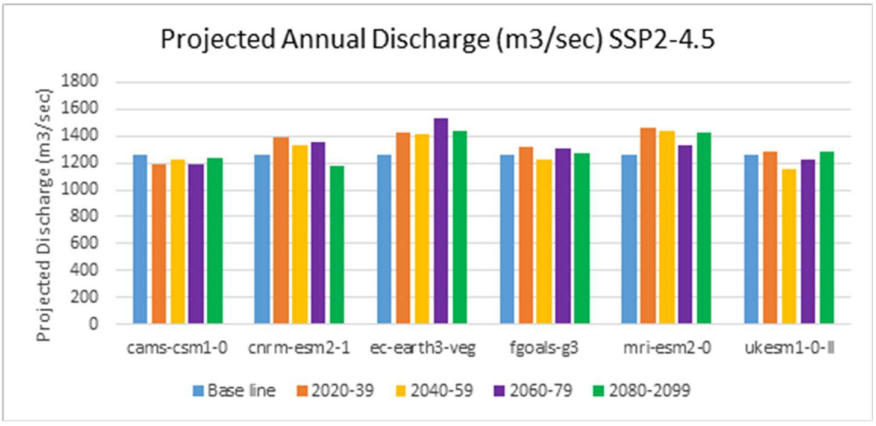

Fig. 9. Average annual Shoran Station flow (2020–2099) for six GCMs under SSP2-4.5.

.

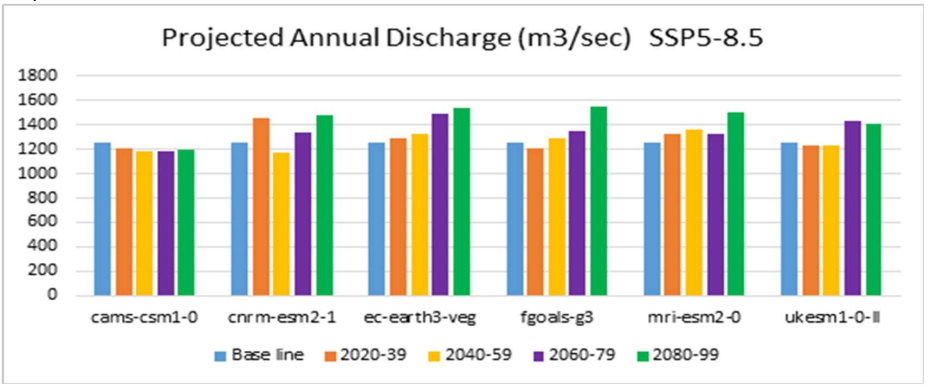

Fig. 20. The average annual Shoran station flow, projected from 2020 to 2099 under the emissions scenario for SSP5-8.5, is derived from the outputs of six general circulation models (GCMs)...

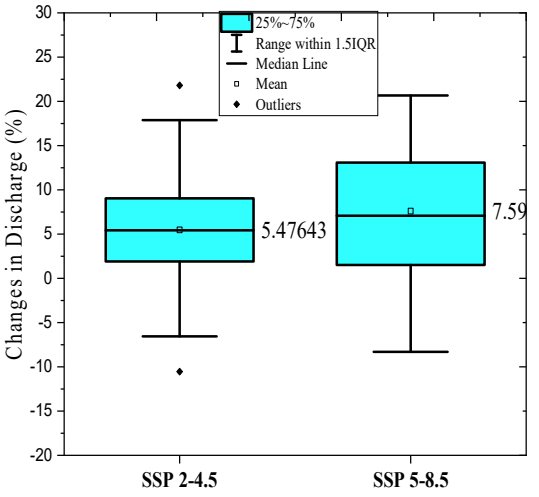

Fig. 13. The amount shift in discharge relative to the baseline is investigated under SSP2-4.5 and SSP5-8.5. nine Global Climate Models (GCMs) in various scenarios.

In Figure 8, (25-75) % of the GCMs used in this study, The SSP5-8.5 emission scenario's highest temperature ranges from 1.6 to 4.15 degrees Celsius, while the SSP2-4.5 emission scenario's maximum temperature ranges from 1.39 to 2.83 degrees Celsius. In SSP5-8.5 emission scenarios, there is also a greater minimum temperature rise. Runoff

and precipitation are closely correlated, meaning that in every circumstance, more rain results in more runoff. variations in temperature only have an indirect impact [47], although there is a positive link [46] between variations in precipitation and basin runoff. The discharge from the Kunhar River Basin is probably going to keep rising, hence future run-of-river hydroelectric projects will need to be planned for. Conclusions On a daily and monthly basis, the runoff was precisely anticipated by the SWAT model. In the calibration and validation stages, the discharge simulation's NSE and R2 values are both greater than 0.75. The cams-csm1-0, miroc6, and ukesm1-0-ll exhibited consistent hydrographs, which makes them more appropriate for use in model validation and calibration. The KRB should anticipate an increase in temperature and precipitation under the various SSPs scenarios. In comparison to the baseline (1990-2020) (figure 6), annual precipitation is predicted to increase by 3.07% (-9.22%, 21.12%) under the SSP2-4.5 emission scenario and by 6.68% (1.61%, 12.75%) under the SSP5-8.5 emission scenario. Under scenarios SSP2-4.5 and For SSP5-8.5, there will be two anticipated increases in maximum air temperatures: Between 0.62 °C and 3.61 °C in 2.09 °C and 0.41 °C and 7.09 °C in 3.07 °C, respectively. The minimum air It is expected that temperatures will increase by 2.09 °C (0.6 °C to 4.58 °C). and by 3.39 °C (1.94 °C to 7.45 °C) respectively. The predicted runoff in the Kunhar River watershed is expected to rise in response to future climate change. Summer runoff may decrease by 13% from the baseline to the end of the century, but winter and spring streamflow may increase by 77.24% (in the mid-future scenario SSP2-4.5) and 40.09% (in the far-mid-future scenario SSP5-8.5). The average annual discharge may rise by 20% It is more probable to drop by ten percent at mid-future (in fgoals under the circumstances SSP2-4.5) than it is in the past (in cnrm-esm2-l) or near (in ec-earth3-veg) (SSP5-8.5).

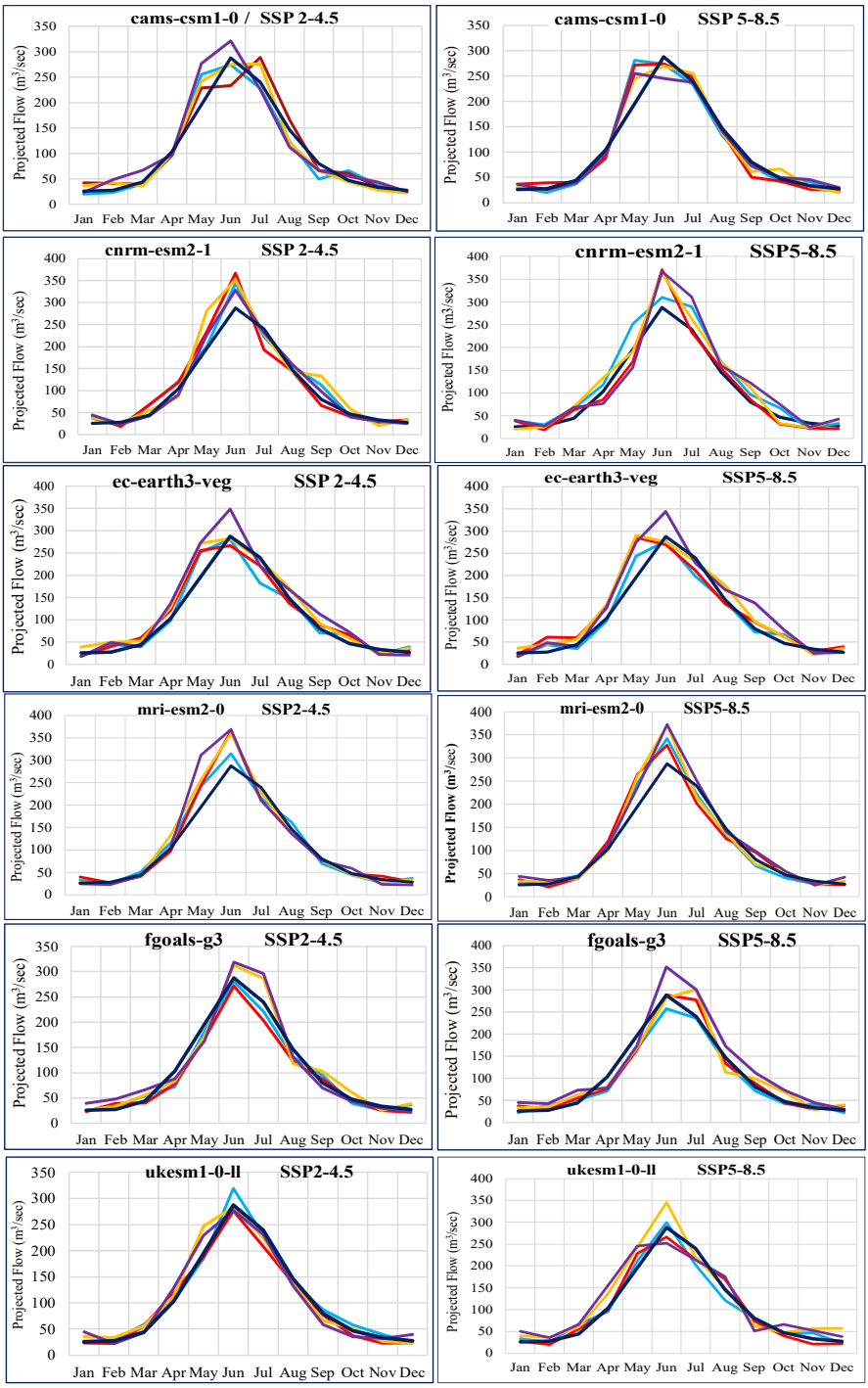

Fig. 42. Flows predicted (m3/month) by six GCMs in the context of CMIP6 emission scenarios.

Additionally, this study offers valuable insights that can help water sector policymakers address Sustainable Development Goals (SDGs) include SDG 6: water quality and hygiene; SDG 13: tackling climate change; and SDG 15: existence on soil [48]. These observations are especially pertinent to the near future. Furthermore, the construction of further run-of-the-river hydroelectric facilities in the area may result in work possibilities for locals [49–51]. This endeavor also contributes to SDG 1.1, which seeks to end extreme poverty worldwide, and is in line with the larger goal of SDG 1 (No Poverty).

References

1. Akhtar, M., N. Ahmad, and M.J.J.J.o.h. Booij, The impact of climate change on the water resources of Hindukush–Karakorum–Himalaya region under different glacier coverage scenarios. 2008. 355(1-4): p. 148-163
2. Tahir, A.A., et al., Modeling snowmelt-runoff under climate scenarios in the Hunza River basin, Karakoram Range, Northern Pakistan. 2011. 409(1-2): p. 104-117.
3. Weart, S.J.B.o.t.a.s., Global warming: How skepticism became denial. 2011. 67(1): p. 41-50.
4. Overland, J.E. and M.J.I.J.o.C. Wang, The 2020 Siberian heat wave. 2021. 41: p. E2341-E2346.
5. Frei, C., et al., Heavy precipitation processes in a warmer climate. 1998. 25(9): p. 1431-1434.
6. Ringler, C. and A.J.W.i. Anwar, Water for food security: challenges for Pakistan. 2013. 38(5): p. 505-514.
7. Dabbous, A., A.J.J.o.I. Tarhini, and Knowledge, Does sharing economy promote sustainable economic development and energy efficiency? Evidence from OECD countries. 2021. 6(1): p. 58-68.
8. Teotónio, C., et al., Assessing the impacts of climate change on hydropower generation and the power sector in Portugal: A partial equilibrium approach. 2017. 74: p. 788-799.
9. Babur, M., et al., Assessment of climate change impact on reservoir inflows using multi climate-models under RCPs—The case of Mangla Dam in Pakistan. 2016. 8(9): p. 389.
10. Azim, F., A.S. Shakir, and A. Kanwal, Impact of climate change on sediment yield for Naran watershed, Pakistan. International Journal of Sediment Research, 2016. 31(3): p. 212-219.
11. Ali, S.S. and S.S. Shah, Climate change impact on flow discharge of Kunhar river catchment using Snowmelt Runoff Model. Journal of Basic & Applied Sciences, 2015. 11: p. 184-192.
12. Mahmood, R., S. Jia, and M.S. Babel, Potential impacts of climate change on water resources in the Kunhar River Basin, Pakistan. Water, 2016. 8(1): p. 23.
13. Akbar, H. and S.H. Gheewala, Changes in hydroclimatic trends in the Kunhar River Watershed. J. Sustain. Energy Environ, 2020. 11: p. 31-41.
14. Weghorst, K.J.B.o.R., Denver, CO, The Reclamation Drought Index: guidelines and practical applications. 1996. 6.

15. Mukhopadhyay, B. and A.J.J.o.H. Khan, A reevaluation of the snowmelt and glacial melt in river flows within Upper Indus Basin and its significance in a changing climate. 2015. 527: p. 119-132.
16. Lv, Z., et al., Effects of recent and potential land use and climate changes on runoff and sediment load in the Upper Yellow River Basin, China. 2020. 29(6): p. 4225-4240.
17. Adnan, M., et al., Snowmelt Runoff Modelling under Projected Climate Change Patterns in the Gilgit River Basin of Northern Pakistan. 2017. 26(2).
18. Musie, M., S. Sen, and I.J.W. Chaubey, Hydrologic responses to climate variability and human activities in Lake Ziway Basin, Ethiopia. 2020. 12(1): p. 164.
19. Reggiani, P., et al., A joint analysis of river runoff and meteorological forcing in the Karakoram, upper Indus Basin. 2017. 31(2): p. 409-430.
20. Soncini, A., et al., Future hydrological regimes in the upper indus basin: A case study from a high-altitude glacierized catchment. 2015. 16(1): p. 306-326.
21. Akbar, H. and S.H.J.J.S.E.E. Gheewala, Changes in hydroclimatic trends in the Kunhar River Watershed. 2020. 11: p. 31-41.
22. Lafon, T., et al., Bias correction of daily precipitation simulated by a regional climate model: a comparison of methods. 2013. 33(6): p. 1367-1381.
23. Arnold, J.G., et al., Large area hydrologic modeling and assessment part I: model development 1. 1998. 34(1): p. 73-89.
24. Arnold, J.G., et al., SWAT: Model use, calibration, and validation. 2012. 55(4): p. 1491-1508.
25. Neitsch, S.L., et al., Soil and water assessment tool theoretical documentation version 2009. 2011, Texas Water Resources Institute.
26. Ahmad, Z., et al., Hydrology of mountainous areas in the upper Indus Basin, Northern Pakistan with the perspective of climate change. 2012. 184: p. 5255-5274.
27. Rahman, K., et al., Streamflow modeling in a highly managed mountainous glacier watershed using SWAT: the Upper Rhone River watershed case in Switzerland. 2013. 27: p. 323-339.
28. Haguma, D., et al., Optimal hydropower generation under climate change conditions for a northern water resources system. 2014. 28: p. 4631-4644.
29. Park, J.Y. and S.J.J.J.o.t.A.W.R.A. Kim, Potential impacts of climate change on the reliability of water and hydropower supply from a multipurpose dam in South Korea. 2014. 50(5): p. 1273-1288.
30. Koycegiz, C. and M.J.W. Buyukyildiz, Calibration of SWAT and two data-driven models for a data-scarce mountainous headwater in semi-arid Konya closed basin. 2019. 11(1): p. 147.
31. Shang, X., et al., Land use and climate change effects on surface runoff variations in the upper Heihe River basin. 2019. 11(2): p. 344.
32. Haider, H., et al., Appraisal of climate change and its impact on water resources of Pakistan: a case study of Mangla Watershed. 2020. 11(10): p. 1071.
33. Iqbal, Z., et al., Evaluation of CMIP6 GCM rainfall in mainland Southeast Asia. 2021. 254: p. 105525.
34. Abbas, A., et al., Evaluation and projection of precipitation in Pakistan using the Coupled Model Intercomparison Project Phase 6 model simulations. 2022. 42(13): p. 6665-6684.
35. Lin, B., Y. Chen, and X.J.J.o.N.R. Chen, A study on regional difference of hydrological parameters of SWAT model. 2013. 28(11): p. 1988-99.
36. Wu, J., H. Zheng, and Y.J.A. Xi, SWAT-based runoff simulation and runoff responses to climate change in the headwaters of the Yellow River, China. 2019. 10(9): p. 509.

37. Abbaspour, K., SWAT-CUP 2012: SWAT Calibration and Uncertainty Programs-A User Manual. Swiss: EAWAG. Retrieved May, 2015. 2014.
38. Akbar, H. and S.H.J.A.J.o.G. Gheewala, Effect of climate change on cash crops yield in Pakistan. 2020. 13: p. 1-15.
39. Moriasi, D.N., et al., Hydrologic and water quality models: Performance measures and evaluation criteria. 2015. 58(6): p. 1763-1785.
40. Gaur, S., A. Bandyopadhyay, and R.J.W.R.M. Singh, From changing environment to changing extremes: Exploring the future streamflow and associated uncertainties through integrated modelling system. 2021. 35: p. 1889-1911.
41. Choi, W., et al., Urbanization and rainfall–runoff relationships in the Milwaukee River basin. 2016. 68(1): p. 14-25.
42. Lu, W., et al., Hydrological projections of future climate change over the source region of Yellow River and Yangtze River in the Tibetan Plateau: A comprehensive assessment by coupling RegCM4 and VIC model. 2018. 32(13): p. 2096-2117.
43. Mahmood, R., S. Jia, and M.S.J.W. Babel, Potential impacts of climate change on water resources in the Kunhar River Basin, Pakistan. 2016. 8(1): p. 23.
44. Nabi, G., et al., Impact of spatial and temporal changes in climate on the Kunhar River Watershed, Pakistan. 2022. 15(15): p. 1311.
45. Bock, L., et al., Quantifying progress across different CMIP phases with the ESMValTool. 2020. 125(21): p. e2019JD032321.
46. Sun, J., et al., Investigating Impacts of Climate Change on Runoff from the Qinhuai River by Using the SWAT Model and CMIP6 Scenarios. 2022. 14(11): p. 1778.
47. Liu, J., B. Xue, and Y.J.S. Yan, The assessment of climate change and land-use influences on the runoff of a typical coastal basin in Northern China. 2020. 12(23): p. 10050.
48. Yin, C., W. Zhao, and P. Pereira, Soil conservation service underpins sustainable development goals. Global Ecology and Conservation, 2022. 33: p. e01974.
49. Perera, A. and U. Rathnayake, Impact of climate variability on hydropower generation in an un-gauged catchment: Erathna run-of-the-river hydropower plant, Sri Lanka. Applied Water Science, 2019. 9(3): p. 57.
50. Khaniya, B., et al., Projection of future hydropower generation in samanalawewa power plant, Sri Lanka. Mathematical Problems in Engineering, 2020. 2020: p. 1-11.
51. Ekanayake, P., et al., Regression-based prediction of power generation at samanalawewa hydropower plant in Sri Lanka using machine learning. Mathematical Problems in Engineering, 2021. 2021: p. 1-12.